



The University of
Nottingham

UNITED KINGDOM · CHINA · MALAYSIA

Rodriguez Gutierrez, D. and Manita, M. and Jaspan, T. and Dineen, Robert A. and Grundy, Richard G. and Auer, Dorothee P. (2013) Serial MR diffusion to predict treatment response in high-grade pediatric brain tumors: a comparison of regional and voxel-based diffusion change metrics. *Neuro-Oncology*, 15 (8). pp. 981-989. ISSN 1523-5866

Access from the University of Nottingham repository:

<http://eprints.nottingham.ac.uk/38889/1/Serial%20MR981.full.pdf>

Copyright and reuse:

The Nottingham ePrints service makes this work by researchers of the University of Nottingham available open access under the following conditions.

This article is made available under the Creative Commons Attribution licence and may be reused according to the conditions of the licence. For more details see:

<http://creativecommons.org/licenses/by/2.5/>

A note on versions:

The version presented here may differ from the published version or from the version of record. If you wish to cite this item you are advised to consult the publisher's version. Please see the repository url above for details on accessing the published version and note that access may require a subscription.

For more information, please contact eprints@nottingham.ac.uk

Serial MR diffusion to predict treatment response in high-grade pediatric brain tumors: a comparison of regional and voxel-based diffusion change metrics

Daniel Rodriguez Gutierrez, Muftah Manita, Tim Jaspan, Robert A. Dineen, Richard G. Grundy, and Dorothee P. Auer

Division of Radiological and Imaging Sciences, University of Nottingham (D.R.G., M.M., R.A.D., D.P.A.), Nottingham University Hospital Trust (T.J.), and The Children's Brain Tumor Research Centre, University of Nottingham, Nottingham, United Kingdom (D.R.G., T.J., D.P.A., R.G.G.)

Background. Assessment of treatment response by measuring tumor size is known to be a late and potentially confounded response index. Serial diffusion MRI has shown potential for allowing earlier and possibly more reliable response assessment in adult patients, with limited experience in clinical settings and in pediatric brain cancer. We present a retrospective study of clinical MRI data in children with high-grade brain tumors to assess and compare the values of several diffusion change metrics to predict treatment response.

Methods. Eighteen patients (age range, 1.9–20.6 years) with high-grade brain tumors and serial diffusion MRI (pre- and posttreatment interval range, 1–16 weeks posttreatment) were identified after obtaining parental consent. The following diffusion change metrics were compared with the clinical response status assessed at 6 months: (1) regional change in absolute and normalized apparent diffusivity coefficient (ADC), (2) voxel-based fractional volume of increased (fiADC) and decreased ADC (fdADC), and (3) a new metric based on the slope of the first principal component of functional diffusion maps (fDM).

Results. Responders ($n = 12$) differed significantly from nonresponders ($n = 6$) in all 3 diffusional change metrics demonstrating higher regional ADC increase, larger fiADC, and steeper slopes ($P < .05$). The slope

method allowed the best response prediction ($P < .01$, $\eta^2 = 0.78$) with a classification accuracy of 83% for a slope of 58° using receiver operating characteristic (ROC) analysis.

Conclusions. We demonstrate that diffusion change metrics are suitable response predictors for high-grade pediatric tumors, even in the presence of variable clinical diffusion imaging protocols.

Keywords: ADC, fDM, pediatric tumor, response prediction, serial diffusion.

Current assessment of CNS tumor treatment response is based on evaluating changes in tumor size several weeks or months after the end of the treatment course. Tumor size is generally estimated from anatomical CT or MRI images,^{1,2} but volume changes can occur relatively late than other physiological changes that may indicate tumor response at an earlier stage. Furthermore, reduction in the proportion of active tumor cells during treatment may not necessarily correlate with lesion dimensions, because there may be areas of edema and necrosis.³ Therefore, significant effort is being applied in the development and validation of functional imaging markers for early response assessment, such as changes in tumor metabolites, diffusion, or perfusion characteristics.^{4–6}

Diffusion MRI is a widely used technique for both diagnosis and treatment response. Regional apparent diffusion coefficient (ADC) changes, estimated from pre- and posttreatment regions of interest (ROIs), have been proposed to predict tumor response to radiation/chemotherapy, with increased ADC associated with

Received November 28, 2012; accepted February 15, 2013.

Corresponding Author: Dorothee Auer, MD, Division of Radiological and Imaging Sciences, Room W/B 1441, Queens Medical Centre, Derby Rd., Nottingham NG7 2UH, UK (dorothee.auer@nottingham.ac.uk).

a more favorable clinical course.^{7–10} In the limited pediatric literature, decreased diffusion has been reported in nonresponding diffuse intrinsic brainstem gliomas (after an initial increase due to radio-therapy effects)^{11,12} and nonresponding medulloblastomas.¹³

Alternatively, individual pixel-to-pixel ADC comparisons may provide a more accurate description of tumor progression by accounting for regional heterogeneity. Several studies have investigated the value of functional diffusion maps (fDMs) in predicting tumor response in adult tumors, time to progression (TTP), and overall survival (OS) after cytotoxic or anti-angiogenic therapies.^{4,7,14,15} Typically, the 2 imaging biomarkers extracted from fDMs are relative volumes exhibiting a decrease^{16,17} and an increase^{4,18} in ADC. This requires selecting a threshold level that defines what constitutes an increase or a decrease in ADC. Several studies have investigated empirically what threshold values may best separate responders from nonresponders, ranging from 0.25 to $0.75 \times 10^{-3} \text{ mm}^2/\text{s}$.^{4,7,14,16} Apart from the choice of threshold, there are other technical factors that may affect the calculation of fDM and regional ADC metrics, including image processing steps, such as registration,¹⁹ and the specifics of ROI selection.¹⁶ Furthermore, the majority of fDM and regional serial ADC analyses published thus far are single-center prospective studies using consistent imaging protocols and identical scanners, often limited to a single tumor type. In clinical practice, however, it is common to encounter different acquisition protocols and scanners among patients and variation in intervals between follow-up scans. All these factors may confound response prediction.

Here, we present the first study, to our knowledge, that investigates and compares the robustness and suitability of several diffusion change metrics for assessment of treatment response on highly heterogeneous clinical pediatric data. We investigate the effects that different ROI selection, registration technique, and threshold selection have on fDM metrics and compare these 2 regional metrics. Finally, we present a new postprocessing method that avoids empirical threshold selection for fDM analysis by using a Principal Component Analysis (PCA) on the scatter of pre- and posttreatment pixel-by-pixel ADC values to infer changes of diffusion heterogeneity. This new approach removes the need to estimate the fDM threshold and may help to provide a simpler and robust tool to assess response.

Materials and Methods

Patients

All patients participating in this study signed informed consent to have their data collected and used for research by the UK Child Cancer and Leukaemia Group (CCLG) Functional Imaging Group database, a UK National Health Service (NHS) Research Ethics Committee-approved study. Eighteen patients with high-grade tumors (World Health Organization [WHO] grade III

and IV) were included (age range, 1.9–20.6 years) who had undergone 2 diffusion MR scans before (0.1–6.3 weeks) and after (1–16 weeks) the start of chemotherapy/radiotherapy as part of clinical care. All patients had diagnosis confirmed by histology, except for one patient with a secreting germ cell tumor, as reviewed by 2 neuro-pathologists with >15 years of experience. Only patients with residual disease were included and, thus, excluded any macroscopic complete resection. Response was defined at 6 months after the beginning of treatment, using combined clinical and radiological criteria according to new Response Assessment in Neuro-Oncology (RANO) criteria²⁰ assessed by an experienced pediatric oncologist (R.G.) and neuro-radiologists (T.J., R.A.D., or D.P.A.). All patients received standard clinical treatment (Table 1).

MRI

Clinical MRI scans were obtained before and after chemotherapy and/or radiotherapy as part of clinical care. The first scan was always performed before the beginning of treatment and/or biopsy. MRI scans were performed on 1 of 3 scanners, a 1.5T GE Sigma (General Electric Medical Systems, Milwaukee, WI), a 1.5T Philips Intera, or a 3T Philips Achieva (Philips Medical Systems, Best, Netherlands), and as part of a multimodal MRI protocol, that consisted of at least pre- and postcontrast axial T1-weighted (TR = [598–647] ms, TE = [12–14] ms $0.45 \times 0.45 \times 4 \text{ mm}^3$ voxel size), precontrast axial T2-weighted (TR = [3000] ms, TE = [72–85] ms $0.45 \times 0.45 \times 4 \text{ mm}^3$ voxel size), and diffusion imaging. Diffusion data were obtained with different sequences, ranging from diffusion-weighted imaging (DWI) to 15-direction diffusion-tensor imaging (DTI), using $b = 0 \text{ s/mm}^2$ and either $b_{\text{max}} = 1000 \text{ s/mm}^2$ or $b_{\text{max}} = 800 \text{ s/mm}^2$, TR = [4883–5800] ms, TE = [59–89] ms, and voxel size of either 12 mm^3 ($2 \times 2 \times 3$) or 14.4 mm^3 ($1.9 \times 1.9 \times 4$).

Additional volunteer data were acquired for each diffusion sequence and used to determine specific fDM thresholds for each combination of pre-post treatment scan protocol.

MRI Protocol Comparison

The effect of using different pre- and posttreatment imaging protocols on diffusion metrics was investigated for 6 of the cases, in which 2 distinct ADC imaging protocols were available for one time point by comparing the respective diffusion distributions in both tumor and white matter (WM) ROIs.

Manual Tracing of Tumor

Pre- and posttreatment whole-tumor ROIs were manually drawn on measurable tumors (ie, >1 cm) by an experienced neuro-radiologist (R.A.D.) and a second experienced researcher (M.M.) using NeuROI (The University of Nottingham, UK; <http://www.nottingham.ac.uk/>

Table 1. Patient demographic characteristics, histopathological tumor diagnosis, and treatment details

Age (years)	Gender	Tumor type	Grade	Type of surgery	Treatment (within scan window)	Scan interval (weeks) ¹	Volume change (at 6 months)	New lesions (at 6 months)	RANO response (at 6 months)	Clinical course after end of therapy
10.7	F	Secr. Germ Cell Tumor		none	Chemotherapy/RT	2.4	decrease	N	PR	No Relapse
2.7	F	PNET	IV	biopsied	Chemotherapy (COG 921)	15.1	no change	N	PD	Death
11.7	M	Pineoblastoma	IV	biopsied	Chemotherapy (PNET3)	4.0	decrease	N	PR	No Relapse
8	M	Pineal PNET	III	biopsied	Chemotherapy (PNET3)	6.9	decrease	N	PR	No Relapse
15	M	Germinoma	III	biopsied	Radiotherapy	6.4	decrease	N	CR	No Relapse
15.8	F	Glioneuronal tumour	IV	debulking	Chemotherapy (Milan)	9.7	decrease	N	SD	Residual Thalamic tumour
4.6	F	DIPG(GBM)	IV	biopsied	Chemotherapy/RT (TMZ)	10.0	no change	N	PD	Death
7.8	F	DIPG(GBM)	IV	biopsied	Chemotherapy/RT (TMZ)	16.7	increase	N	PD	Death
3.5	F	MB	IV	debulking	Chemotherapy (Milan)	4.3	decrease	N	CR	Leptomeningeal spread
1.9	M	MB	IV	biopsied	Chemotherapy (PNET3)	4.1	decrease	N	PR	Death
6.2	M	DIPG (Glioblastoma)	III	biopsied	Chemotherapy/RT (TMZ)	13.1	increase	N	PD	Death
4.7	M	MB	IV	debulking	Chemotherapy/RT (POG 9031)	3.4	decrease	Y	PR	Supra tentorial recurrent tumour
9.2	M	MB	IV	debulking	Chemotherapy (Milan)	1.9	decrease	N	CR	No Relapse
12.3	M	Germinoma	III	biopsied	Chemotherapy	2.1	decrease	N	PR	No Relapse
12.4	M	GBM	IV	debulking	Chemotherapy/RT (TMZ)	16.9	decrease	N	PR	Death
6.8	M	MB	IV	biopsied	Chemotherapy/RT (POG 9031)	10.0	decrease	N	PR	No Relapse
20.6	M	Glioblastoma(GBM)	IV	biopsied	Chemotherapy (TMZ)	12.6	decrease	N	SD	No Relapse
12.8	F	MB	IV	debulking	Chemotherapy (Milan)	11.3	decrease	N	PR	No Relapse
11.2	F	Pineoblastoma	IV	biopsied	Chemotherapy (PNET3)	8.9	decrease	N	PR	No Relapse

Abbreviations: COG, Children's Oncology Group; CR, complete response; DIPG, diffuse intrinsic pontine glioma; GBM, glioblastoma multiforme; MB, medulloblastoma; PD, progressive; PNET, primitive neuroectodermal tumor; POG, Pediatric Oncology Group; PR, partial response; RANO, Response Assessment in Neuro-Oncology; RT, radiotherapy; SD, stable disease; TMZ, temozolomide.

scs/divisions/clinicalneurology/software/neuroi.aspx). Previous studies have used either contrast-enhancing tissue or abnormal FLAIR areas to define the ROIs, but it is unclear which is a better predictor of OS.^{16,19} In this study, tumor tissue was defined on the contrast-enhanced T1w images as areas of abnormal enhancement, but also using the coregistered precontrast T2w images to identify and exclude blood vessels adjacent to enhancing tumor and to include low-contrast tumor or necrotic tissue adjacent to edema. This allowed comparing tumor volumes, including enhancing and nonenhancing tumor parts, by multiplying the areas from these ROIs with inter-slice distances.

Regional ADC Change Metrics

ADC change was calculated from the ROIs generated for fDM analysis (see below). Change was expressed as the post- / pre ratio of mean tumor ADC (ADC_r) computed for each lesion. WM-normalized ratios (nADC_r) were computed using a small reference region in normal-appearing WM. The advantage of using normalized ADC is to remove some of the heterogeneity that the use of different scanners and protocols introduces. The disadvantages of this normalization are introducing an unwanted age dependence in the very young patients and potential bias from disease and treatment effect on

WM that cannot be avoided by choosing normal-appearing WM (2 of the 18 cases were in recurrent patients). To better interpret fDM, we also derived peak height decrease (PkDec) as a heterogeneity measure from normalized tumor histograms.

Generating Functional Diffusion Maps

The process of generating a fDM involves a series of sequential processing steps. First, data registration is performed; all pre- and postcontrast data are registered to a common baseline image (typically anatomic, such as FLAIR, T2w, or contrast-enhanced T1w). This step may include linear or nonlinear registration processes. Second, tumor ROIs are defined; these are delineated on the basis of the anatomical images and applicable to the registered diffusion data. Third, the fDM is calculated using a predefined threshold that determines a suitable change in ADC values; pixel-by-pixel change is classified as increase, no change, or decreased ADC. Finally, fDM metrics, such as overall volumes of decrease or increase in ADC, are calculated.

All aforementioned steps contain operator dependencies that may affect the final fDM metrics. Different tests and processes to assess and minimize the effect of these are presented below.

fDM Preprocessing: Registration and ROI Definition

All images (both pre- and posttreatment) were spatially coregistered to the pretreatment T2w images with use of a mutual information-based affine registration using FSL's linear registration tool (FLIRT; FMRIB, Oxford, UK; <http://www.fmrib.ox.ac.uk/fsl/>).

Using the same ROIs according to the regional ADC analysis, 2 types of ROI combinations and registration were compared for the fDM approach: (1) a combined ROI from those pixels only included in both pre- and posttreatment-ROIs and (2) pretreatment ROI only—in this case, the affine registration was followed by an additional nonlinear registration step of the posttreatment diffusion data, also using FSL. The standard settings of FSL's nonlinear registration tool (FNIRT) were used for comparability with previous studies.¹⁹

fDM Metrics

fDMs were computed using in-house software developed in MATLAB R2010a (The MathWorks Inc., Natick, MA, 2010). The fraction of decreased (fdADC) and the fraction of increased (fiADC) ADC were determined in accordance with methods in previous studies.^{4,15,18} In addition to fiADC and fdADC, we used their ratio $fDMratio = fiADC / (0.01 + fdADC)$, with the 0.01 factor introduced to avoid division by zero in those cases in which there were no decreased diffusion voxels. All the aforementioned metrics were also computed for normalized ADC, as described above, to produce corresponding normalized versions: nfiADC, nfdADC, and nfdMratio.

fDM Thresholds

Although ADC thresholds ranging from 0.25 to $0.75 \times 10^{-3} \text{ mm}^2/\text{s}$ have been investigated, previous studies have mostly used 0.5 or $0.4 \times 10^{-3} \text{ mm}^2/\text{s}$ ^{4,7,15,18,19,21,22} to define the no-change ADC level. In addition to these 2 standard thresholds and to assess the effect of heterogeneous imaging protocols that contained different scanners, resolution, slice thickness, or diffusion gradient directions, individual fDM thresholds were computed for each possible protocol combination, based on the minimum detectable ADC changes of healthy volunteer data. This allowed us to determine protocol-pair specific thresholds that showed no ADC change for 90%, 95%, and 98% of pixels in a skull-stripped whole-brain ROI. The range and mean values for these thresholds were 0.2–0.5/ $0.4 \times 10^{-3} \text{ mm}^2/\text{s}$ (90%), 0.3–0.8/ $0.6 \times 10^{-3} \text{ mm}^2/\text{s}$ (95%), and 0.5–0.9/ $0.8 \times 10^{-3} \text{ mm}^2/\text{s}$ (98%). For same-protocol combinations, the minimum detectable thresholds were similar to the literature,²³ and they increased for mixed-protocols. For the normalized version of the fDM metrics, all above threshold values were normalized using the same method as for the data itself.

A further modification of the fDM approach, the graded fDM proposed by Ellingson,¹⁶ was also tested. In graded fDMs, both decreasing and increasing diffusion volumes are subclassified into 3 bins: [0.25 to 0.4, 0.4 to 0.75, above 0.75] $\times 10^{-3} \text{ mm}^2/\text{s}$ for increased diffusion and [–0.25 to –0.4, –0.4 to –0.75, below –0.75] $\times 10^{-3} \text{ mm}^2/\text{s}$ for decreased diffusion.

Nonthresholded Functional Diffusion Maps

To avoid the problem of empirical fDM threshold selection, we analyzed the pre- and posttreatment ADC scatter plot (Fig. 1). This scatter plot has been used previously to show the concept of fDMs, but we are the first to analyze it quantitatively. The 2D distribution of this scatter plot holds information on tumor heterogeneity and its change, and the direction of largest variance can be computed by PCA. PCA defines orthogonal linear combinations of variables, principal components (PC), which describe the largest amount of variability in the data. In the case of change in pre- and posttreatment ADC values, the first principal component can be used to determine whether the largest variability in ADC values occurs before or after treatment. If the direction of the first principal component describes the same variability before and after treatment (ie, a line $y = mx$ with a slope m of 1, or an angle of 45°), it indicates no change in heterogeneity of ADC values (ie, the spread of ADC values would have been unaffected by treatment). A higher slope for the first PC indicates an increase in heterogeneity, and a lower slope indicates a decrease in heterogeneity. Therefore, we used the angle of the slope of the first PC on a pre- and posttreatment ADC change scatter plot to calculate the change in tumor ADC heterogeneity (Fig. 2).

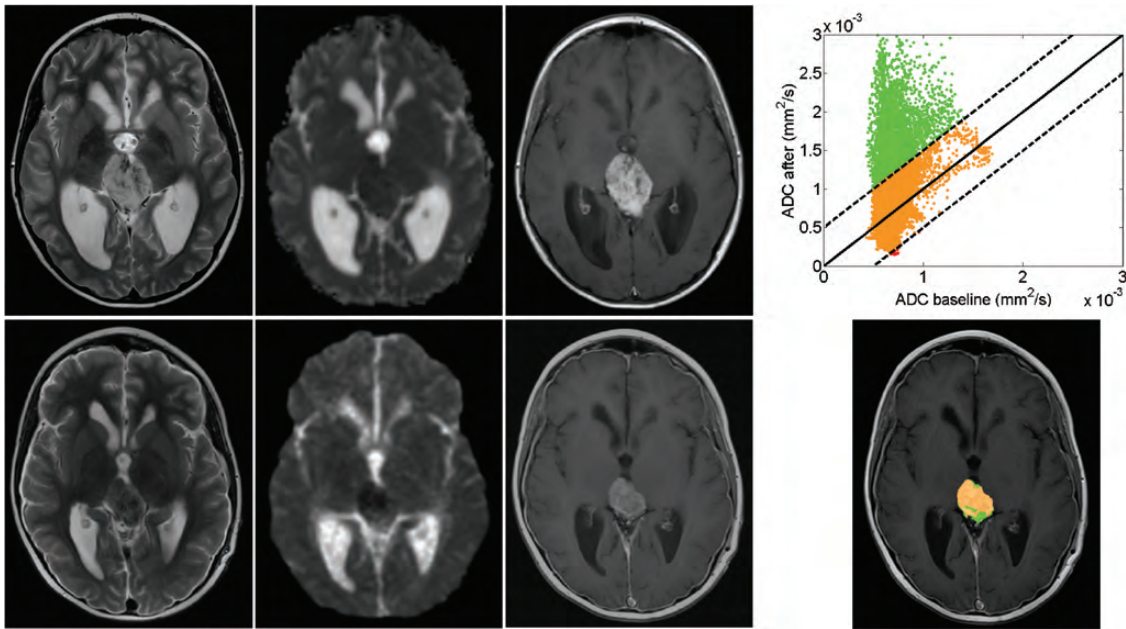


Fig. 1. Serial MRI in a patient with pineoblastoma showing partial response to chemotherapy. Top row corresponds to pretreatment and bottom row to posttreatment (1 month) scan data. Left 3 columns: T2, diffusion-weighted and contrast-enhanced T1 images. Right column: fDM scatter plot for each voxel in the ROI (top) and fDM map (bottom); green voxels indicate an increase in diffusion, red voxels indicate a decrease in diffusion, and orange voxels indicate no change.

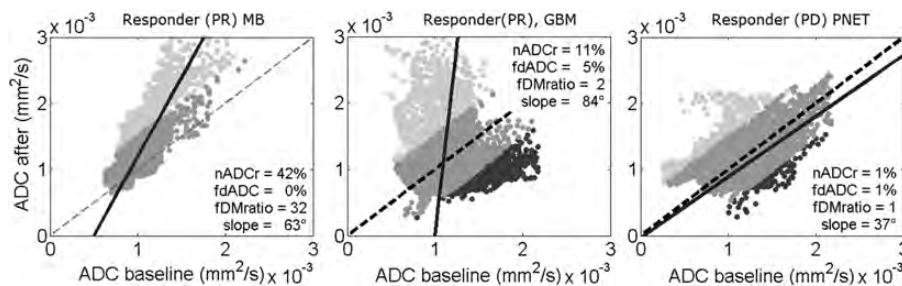


Fig. 2. fDM scatter plots with direction of first principal component (solid line). Left: fDM for a responding MB, showing a first principal component with high slope, compared with the diagonal (dotted line). Middle: fDM for a responding GBM, showing a first principal component with high slope, and conventional fDM analysis shows a substantial volume of decreased diffusion (dark grey pixels). Right: fDM for a nonresponding PNET, showing a first principal component with low slope. Light gray voxels indicate an increase in diffusion, dark gray voxels indicate a decrease in diffusion, and medium gray voxels indicate no change.

Statistical Analysis

Statistical analysis was performed using PASW Statistics 18, release version 18.0.0 (SPSS, Inc.). Paired t tests were used to compare differences between both tumor and WM. ADC values calculated using the same imaging protocol differed with those calculated using different pre- and posttreatment protocols. Candidate marker distributions were tested for normality and homogeneity of variance with use of Shapiro-Wilk and Levene's test. Nonnormally distributed fDM candidate response markers were transformed to normal distributions with use of log transformation ($Y_T = \log_{10} [Y + 1]$). Analysis of covariance was used to test for differences in candidate biomarkers between responders and nonresponders, using age as covariate. The significance level

was defined as $P < .05$. Effect sizes were calculated as partial-eta squared (η^2). ROC curves were used to determine the best threshold for separating responders and nonresponders for the slope method.

Results

Quality Control

Differences between fDM analysis for both observers (M.M. and R.D.) were small, with single-measure intraclass correlation coefficient for either fiADC or fdADC > 0.97 on any of the threshold levels. Similarly, the intraclass correlation coefficient for ADCr was 0.94.

Table 2. Differences between responders and nonresponders in patient demographic characteristics and regional diffusion candidate biomarkers.

Variable	Responders mean \pm SD, or mean [range]	non-responders mean \pm SD, or mean [range]	P	η^2
Age (years)	9.1 (\pm 4.1)	9.6 (\pm 7.0)	NS	–
Scan time (weeks after treatment)	6.4 [1.0–16.2]	6.9 [2.4–12.3]	NS	–
Volume decrease (%)	33 (\pm 35)	25 (\pm 21)	NS	–
Baseline ADC ($\times 10^{-3}$ mm ² /s)	1.0 (\pm 0.2)	1.1 (\pm 0.2)	NS	–
Baseline nADC	1.2 (\pm 0.2)	1.5 (\pm 0.2)	NS	–
ADCr (% increase)	30 (\pm 27)	2 (\pm 19)	0.08	–
nADCr (% increase)	35 (\pm 23)	3 (\pm 16)	0.03	0.38

Significance and effect size (for significant candidate biomarkers only). Abbreviations: ADCr, ADC ratio; η^2 , partial eta squared if significant; nADC, normalized ADC; nADCr, normalized ADC ratio; NS, not significant.

Table 3. Bestperforming fDM-based candidate biomarkers (with nfiADC and nfDMratio calculated using a 0.4×10^{-3} mm²/s threshold [normalized], affine registration and pre- and posttreatment ROIs).

Candidate biomarker	Responders mean (\pm SD)	Non-responders mean (\pm SD)	P	η^2
nfiADC	37.0 (\pm 23.9)	10.5 (\pm 8.4)	.02	0.30
nfDMratio	14.4 (\pm 11.8)	1.0 (\pm 1.2)	.01	0.51
Slope	75.9° (\pm 12.8°)	47.4° (\pm 7.8°)	.01	0.76

Slope method was calculated using normalized ADC. Abbreviations: η^2 , partial eta squared; nfDMratio, normalized fDMratio; nfiADC, fraction of increased normalized ADC.

Regional ADC measures derived from different protocols acquired during the same scan (6 pairs) did not differ significantly (mean difference [range] for tumor: 0.02×10^{-3} mm²/s [0.005 – 0.34] $\times 10^{-3}$ and for WM 0.01×10^{-3} mm²/s [0.002 – 0.23] $\times 10^{-3}$).

Treatment Effect

Tumor volumes significantly decreased by a mean of 30% from baseline (mean [range] 26.0 cm³ [3.5–60.1]) to the posttreatment scan (17.6 cm³, range [1.8–49.8]; paired *t* test *P* < .05). There was an overall increase in diffusion due to treatment, with an ADCr increase (mean \pm SD) of 24% \pm 25% and an nADCr increase of 26% \pm 20%.

Response Prediction

At 6 months after treatment, 12 patients were classed as responders (complete or partial response) and 6 as nonresponders (stable or progressive disease) (Table 1). At this time, the observed tumor volume decrease was not significantly different (Mann-Whitney, *P* > .05) between responders and nonresponders (Table 2). Baseline ADC measures (mean ADC and normalized mean ADC) were not significantly different between responders and nonresponders (*P* > .05).

Both ADCr and nADCr were higher in responders than in nonresponders. This increase was significant

in nADCr (*P* = .03) and not significant in ADCr (Table 2).

Conventional fDMs

The best fDMratio to differentiate between responders and nonresponders (*P* = .01) was found using the fixed threshold of 0.4×10^{-3} mm²/s, affine registration, a combined pre-/post-treatment ROI, and normalized ADC (Table 3). fDMratio proved to be robust against use of different threshold levels (using either the variable 98% or 0.4 or 0.5×10^{-3} mm²/s), registration method, and ADC normalisation (Table 4). ROC analysis suggested an optimum threshold <2.0 for identifying nonresponse to treatment using fDMratio (sensitivity = 78%, specificity = 83%). The best fiADC (*P* = .02) was also obtained using the 0.4×10^{-3} mm²/s threshold, normalized ADC, but nonlinear registration. fiADC results were more dependent on image processing than fDMratios (Table 4).

fdADC was mostly unable to significantly differentiate between responders and nonresponders, as were the candidate biomarkers calculated using the variable 90% and 95% thresholds (Table 4).

Similarly, none of the 6 metrics based on volumes of diffusion change (3 decreasing and 3 increasing subvolumes) for the graded fDM approach significantly differentiated between responders and nonresponders (*P* > .05).

Slope of Nonthresholded fDMs

The angle of the slope of the first principal component was higher in responders than in nonresponders (Table 3). This difference using normalized ADC was significant (*P* = .01), and the separation between them was clearer than in the thresholded fDM methods (η^2 = 0.76). ROC analysis suggested an optimum threshold <58° for identifying nonresponse to treatment yielding the best accuracy because of slightly better sensitivity than fDMratio (sensitivity = 83%, specificity = 83%). The slope method using nonnormalised ADC performed similarly (*P* = .01, η^2 = 0.68).

Table 4. Functional diffusion mapping for predicting response in pediatric high-grade tumors: effects of different metrics and postprocessing steps.

Threshold ($\times 10^{-3}$ mm ² /s)	ROI/registration	nfiADC		nfdADC		fDMratio		nfDMratio	
		P	η^2	P	η^2	P	η^2	P	η^2
Fixed 0.5	Pre and post/affine	.04	0.26	.36	–	.01	0.48	.01	0.49
	Pre-treat./non-rigid	.05	0.24	.02	0.31	.01	0.42	.01	0.42
Fixed 0.4	Pre and post/affine	.03	0.26	.26	–	.01	0.48	.01	0.51
	Pre-treat./non-rigid	.02	0.30	.55	–	.01	0.42	.01	0.39
Variable 98%	Pre and post/affine	.02	0.28	.39	–	.01	0.45	.01	0.44
	Pre-treat./non-rigid	.06	–	.33	–	.01	0.43	.01	0.46
Variable 95%	Pre and post/affine	.26	–	.73	–	.04	0.23	.05	0.26
	Pre-treat./non-rigid	.08	–	.49	–	.06	–	.07	–
Variable 90%	Pre and post/affine	.43	–	.79	–	.34	–	.34	–
	Pre-treat./non-rigid	.51	–	.64	–	.26	–	.25	–

Significance and effect size (for significant metrics only). Abbreviations: fDMratio, fiADC to fdADC ratio; η^2 , partial eta squared; nfdADC, fraction of decreased normalized ADC; nfDMratio, normalized fDMratio; nfiADC, fraction of increased normalized.

Discussion

We investigated the suitability of various serial diffusion metrics to predict treatment response in children with high-grade brain tumors who had undergone heterogeneous clinical diffusion protocols. Separation of treatment responders and nonresponders was feasible at 8-week intervals with most diffusion metrics, with best results (83% accuracy) achieved for a novel slope of the first principal component followed by the ratio of voxels with increased over decreased diffusion. This suggests that increase in diffusion heterogeneity and preferential increase in diffusivity are associated with treatment response. These results are in line with the scarce previous work in the pediatric literature.^{13,24}

As expected, fDM metrics yielded higher effect sizes than regional ADC changes. Regional ADC changes were only significantly higher in responders than in nonresponders when normalized to white matter. This normalization step was not necessary for significance in the fDM metrics, thus avoiding the introduction of age dependence because of white matter maturation or a nonspecific treatment effect on white matter diffusivity.

fDM Metrics

We found that fDMratio, which combines information from both fdADC and fiADC, produced the best results, compared with previously proposed functional diffusion metrics. fdADC and fiADC results have been published on high-grade tumor gliomas, with changes in fdADC (but not fiADC) indicative of overall survival in patients after cytotoxic or anti-angiogenic treatment.^{15,17} In contrast, fiADC (but not fdADC) has been shown to predict overall survival in the same type of tumor after similar imaging protocols except radiotherapy.^{18,25} One might speculate that a combined marker such as fDMratio might prove to be more robust to treatment type. We confirmed that registration¹⁹ and ROI selection^{16,19} and choice of threshold values¹⁴ can affect the performance of response

prediction. The diagnostic accuracy of the best discriminating metric, fDMratio, was largely unaffected by the different applied methodologies, such as the use of different threshold levels, ROI selection, registration method, or ADC normalization (Table 4).

fDM Thresholds

Both fixed thresholds of 0.5 and 0.4×10^{-3} mm²/s and the variable 98% threshold were sensitive to detecting the clinical response status, and lower variable thresholds (90% and 95%) were not. For the imaging protocol combinations tested here, the 98% threshold reflects individual threshold values of $0.2\text{--}0.5 \times 10^{-3}$ mm²/s. The graded fDM approach suggests that intermediate diffusion decreases at $0.25\text{--}0.4 \times 10^{-3}$ mm²/s would be more sensitive to relevant biological change in tumor cellularity, as opposed to change in nonspecific edema.¹⁶ This could not be replicated in this study (neither for decreased nor increased diffusion subvolumes), perhaps because of a more heterogeneous dataset.

Slope of Nonthresholded fDM

To quantify the information of the fDM scatter plots without using empirical thresholds, we investigated the diagnostic value of the slope of the first principal component. This way, we determined the change in largest data variability, which proved to be the best indicator of treatment response among all the fDM-based methods. The slope of the first PC afforded clinically useful discrimination of 83% with use of an angle of 58° as cutoff. Of importance, prediction of tumor response to treatment with use of nonthresholded fDMs eliminates the need to define a diffusion change threshold, which is dependent on a number of factors that cannot always be controlled and is difficult to generalize. For example, one of the problems with nonrigid registration fDMs is that the literature standard thresholds calculated on nondeformed data¹⁴ should be recalculated using

the nonrigid registration method, because their suitability largely depends on the extent of the deformation that is applied. These thresholds would need to be recalculated for any changes on the deformation parameters or algorithm. The new approach of determining the slope of nonthresholded fDMs eliminates this problem.

Limitations

There are several limitations of the current study. We only studied a small and heterogeneous sample size, a common problem in single-center pediatric studies that reflects the relative low incidence of pediatric brain tumors (~3 per 100 000 children per year).²⁶ This problem is aggravated by heterogeneous tumor types, presence of postsurgical residue, treatment protocols, and follow-up intervals. Thus, our presented findings have to be considered as preliminary but are likely to be more representative of clinical settings and may even address some multi-center scanner and protocol variability. Nevertheless, despite these limitations, we were able to clearly separate responders from nonresponders with a range of serial diffusion metrics. One may speculate that, with more homogeneous image acquisition and tumor type sample, it may be possible to further stratify responders into complete and partial response and nonresponders into stable and progressive disease with use of fDM biomarkers, which was not possible in this dataset.

Moreover, we included datasets relatively long after treatment initiation (median, 9 weeks; range, 1–16 weeks), in contrast to fDM adult studies assessed at 3¹⁸ or 6 weeks.¹⁶ At longer intervals, fDM analysis becomes less relevant as volume reduction in responders becomes visible in conventional MR. Although our study cannot be extrapolated to earlier time points, a previous pediatric study suggested that changes in ADC can predict radiotherapy response as early as one week.¹⁰

An important question for our heterogeneous clinical dataset was to assess and, if need be, control for the effect of using a mix of ADC maps from 15-direction DTI to single-direction DWI. For those patients in whom both different and same pre- and posttreatment protocols were available, the differences in fDM biomarkers were found to be not significant. Because this was only a limited small subgroup of the data, the effect was further investigated by using normalized ADC values and by using fDM thresholds specific to

each pre- and posttreatment protocol. Although standardization of protocols is clearly preferable, our study provides some evidence that mixing of protocols is feasible and did not mask differential treatment effects in relation to clinical response.

There is increasing evidence that diffusion metrics may contribute to differentiate true progression from pseudo-progression. In this study, there were 3 patients with increased enhancing tumor volume who were later classified as responders. Two of these were correctly classed as responders with use of fDM metrics. However, these are only small numbers with variable time intervals and variable treatments, factors that will affect the prevalence and detection of pseudo-progression.

Conclusion

To the best of our knowledge, this is the first study that investigated the use of fDM-based biomarkers of treatment response in pediatric high-grade brain tumors. Even in the presence of clinical and technical heterogeneity, our results suggest that fDM techniques are superior to regional ADC change assessment and provide suitable imaging biomarkers to predict tumor response. A new fDM analysis technique based on the slope of the first principal component yielded the best results with an overall diagnostic accuracy of 83% to separate responders from nonresponders.

Acknowledgments

We thank Rose English, for data collection; James Lowe and Keith Robson, for histopathological analysis; and Gill Glen, for data management.

Funding

This work was supported by the Cancer Research-UK and Engineering and Physical Sciences Research Council Cancer Imaging Programme at the Children's Cancer and Leukaemia Group (CCLG), England (C7809/A10342 and C7809/A10342[in association with the MRC and England Department of Health]).

Conflict of interest statement. None declared.

References

1. Therasse P, Arbutk SG, Eisenhauer EA, et al. New guidelines to evaluate the response to treatment in solid tumors. European Organization for Research and Treatment of Cancer, National Cancer Institute of the United States, National Cancer Institute of Canada. *J Natl Cancer Inst.* 2000;92(3):205–216.
2. Macdonald DR, Cascino TL, Schold SC, Jr., Cairncross JG. Response criteria for phase II studies of supratentorial malignant glioma. *J Clin Oncol.* 1990;8(7):1277–1280.
3. Wahl RL, Jacene H, Kasamon Y, Lodge MA. From RECIST to PERCIST: Evolving Considerations for PET response criteria in solid tumors. *J Nucl Med.* 2009;50(Suppl 1):1225–1505.

4. Moffat BA, Chenevert TL, Lawrence TS, et al. Functional diffusion map: a noninvasive MRI biomarker for early stratification of clinical brain tumor response. *Proc Natl Acad Sci USA*. 2005;102(15):5524–5529.
5. Tsien C, Galban CJ, Chenevert TL, et al. Parametric response map as an imaging biomarker to distinguish progression from pseudoprogression in high-grade glioma. *J Clin Oncol*. 2010;28(13):2293–2299.
6. Vaidya SJ, Payne GS, Leach MO, Pinkerton CR. Potential role of magnetic resonance spectroscopy in assessment of tumour response in childhood cancer. *European Journal of Cancer*. 2003;39(6):728–735.
7. Hamstra DA, Chenevert TL, Moffat BA, et al. Evaluation of the functional diffusion map as an early biomarker of time-to-progression and overall survival in high-grade glioma. *Proc Natl Acad Sci USA*. 2005;102(46):16759–16764.
8. Huang CF, Chiou SY, Wu MF, Tu HT, Liu WS, Chuang JC. Apparent diffusion coefficients for evaluation of the response of brain tumors treated by Gamma Knife surgery. *J Neurosurg*. 2010;113(Suppl):97–104.
9. Li Y, Lupo JM, Polley M-Y, et al. Serial analysis of imaging parameters in patients with newly diagnosed glioblastoma multiforme. *Neuro Oncol*. 2011;13(5):546–557.
10. Mardor Y, Pfeffer R, Spiegelmann R, et al. Early Detection of Response to Radiation Therapy in Patients With Brain Malignancies Using Conventional and High b-Value Diffusion-Weighted Magnetic Resonance Imaging. *Journal of Clinical Oncology*. 2003;21(6):1094–1100.
11. Prabhu SP, Ng S, Vajapeyam S, et al. DTI assessment of the brainstem white matter tracts in pediatric BSG before and after therapy: a report from the Pediatric Brain Tumor Consortium. *Childs Nerv Syst*. 2011;27(1):11–18.
12. Chen HJ, Panigrahy A, Dhall G, Finlay JL, Nelson MD, Jr., Bluml S. Apparent diffusion and fractional anisotropy of diffuse intrinsic brain stem gliomas. *AJNR Am J Neuroradiol*. 2010;31(10):1879–1885.
13. Schubert MI, Wilke M, Muller-Weihrich S, Auer DP. Diffusion-weighted magnetic resonance imaging of treatment-associated changes in recurrent and residual medulloblastoma: preliminary observations in three children. *Acta Radiol*. 2006;47(10):1100–1104.
14. Ellingson BM, Malkin MG, Rand SD, et al. Validation of functional diffusion maps (fDMs) as a biomarker for human glioma cellularity. *Journal of Magnetic Resonance Imaging*. 2010;31(3):538–548.
15. Ellingson BM, Malkin MG, Rand SD, et al. Volumetric analysis of functional diffusion maps is a predictive imaging biomarker for cytotoxic and anti-angiogenic treatments in malignant gliomas. *J Neurooncol*. 2011;102(1):95–103.
16. Ellingson BM, Cloughesy TF, Lai A, et al. Graded functional diffusion map-defined characteristics of apparent diffusion coefficients predict overall survival in recurrent glioblastoma treated with bevacizumab. *Neuro Oncol*. 2011;13(10):1151–1161.
17. Ellingson BM, Cloughesy TF, Zaw T, et al. Functional diffusion maps (fDMs) evaluated before and after radiochemotherapy predict progression-free and overall survival in newly diagnosed glioblastoma. *Neuro Oncol*. 2012;14(3):333–343.
18. Hamstra DA, Galban CJ, Meyer CR, et al. Functional diffusion map as an early imaging biomarker for high-grade glioma: correlation with conventional radiologic response and overall survival. *J Clin Oncol*. 2008;26(20):3387–3394.
19. Ellingson BM, Cloughesy TF, Lai A, Nghiemphu PL, Pope WB. Nonlinear registration of diffusion-weighted images improves clinical sensitivity of functional diffusion maps in recurrent glioblastoma treated with bevacizumab. *Magnetic Resonance in Medicine*. 2012;67(1):237–245.
20. Wen PY, Macdonald DR, Reardon DA, et al. Updated response assessment criteria for high-grade gliomas: response assessment in neuro-oncology working group. *Journal of Clinical Oncology*. 2010;28(11):1963–1972.
21. Lee KC, Bradley DA, Hussain M, et al. A feasibility study evaluating the functional diffusion map as a predictive imaging biomarker for detection of treatment response in a patient with metastatic prostate cancer to the bone. *Neoplasia*. 2007;9(12):1003–1011.
22. Moffat BA, Chenevert TL, Meyer CR, et al. The functional diffusion map: an imaging biomarker for the early prediction of cancer treatment outcome. *Neoplasia*. 2006;8(4):259–267.
23. Harris AD, Govindaraj M, Frayne R. Minimum detectable difference of MR diffusion maps in acute ischemic stroke. *Journal of Magnetic Resonance Imaging*. 2008;27(3):629–633.
24. Chenevert TL, Stegman LD, Taylor JMG, et al. Diffusion magnetic resonance imaging: an early surrogate marker of therapeutic efficacy in brain tumors. *Journal of the National Cancer Institute*. 2000;92(24):2029–2036.
25. Galban CJ, Chenevert TL, Meyer CR, et al. Prospective analysis of parametric response map-derived MRI biomarkers: identification of early and distinct glioma response patterns not predicted by standard radiographic assessment. *Clin Cancer Res*. 2011;17(14):4751–4760.
26. Arora RS, Alston RD, Eden TO, Estlin EJ, Moran A, Birch JM. Age-incidence patterns of primary CNS tumors in children, adolescents, and adults in England. *Neuro Oncol*. 2009;11(4):403–413.